Chapter 5

TYPE I HUMAN AUDITORY NERVE FIBRE MODEL

A preliminary study of the results presented in this chapter was presented at:
South African Institute for Physics 52nd Annual Conference, University of The Witwatersrand, Johannesburg, July 3 - 6, 2007

Conference proceedings will be published in the South African Journal of Science:
Smit, J. E., Hanekom, T. and Hanekom, J. J. (2008) Predicting human auditory action potential characteristics through modification of the Hodgkin-Huxley equations, *accepted for publication*

5.1 INTRODUCTION

Even though the physical structure of human ANFs has been investigated (Nadol Jr, 1988; Nadol Jr, 1990; Nadol Jr *et al.*, 1990; Rosbe *et al.*, 1996; Zimmermann *et al.*, 1995; Glueckert *et al.*, 2005a; Glueckert *et al.*, 2005c), the properties and types of ionic membrane currents of spiral ganglion cells have been characterised in murine (Mo *et al.*, 2002; Reid *et al.*, 2004; Hossain *et al.*, 2005; Chen and Davis, 2006) and guinea-pig (Bakondi *et al.*, 2008), but not in human. It is therefore only possible to hypothesise that since the ANF is of the sensory type, the possibility exists that similar ionic membrane currents to those found in a peripheral sensory fibre might be present.

In this chapter the general human sensory nerve fibre model is incorporated into the

Rattay *et al.* (2001b) ANF model. The axonal morphological parameters are changed to a Type I peripheral ANF and the model coupled to a volume conduction model of the cochlea. The objective of this chapter is to determine if this modified model can predict the excitability behaviour of the human peripheral auditory system betterthan previous ANF models and hence if the abovementioned hypothesis holds.

5.2 MODEL AND METHODS

5.2.1 The auditory nerve fibre model

The Type I human ANF model was based on the ANF cable model by Rattay *et al.* (2001b), but with the axon replaced with the generalised human sensory nerve fibre model described in Chapter 4. The dendrite and axon are divided into cylindrical compartments, while the soma is assumed to be spherical (Rattay *et al.*, 2001b). The nerve fibre morphometry is shown in Figure 5.1. An additional modification to the ANF model was a shortening of the dendrite to fit the somal position of its counterpart in the volume conduction cochlear model. Two types of Type I spiral ganglion cells exist with somal diameters varying between 24.6 μm and 29.9 μm (Schuknecht, 1993; Rosbe *et al.*, 1996). A value of 27.0 μm was thus assumed in the model.

Nodes of Ranvier were unmyelinated active axolemmae with only the axonal nodes utilising the human Ranvier node model described in Chapter 3. The myelinated axonal internodes were simple double cable structures as modelled by Blight (1985) and described in Chapter 4. SEM photographs and measured data of human auditory myelinated large Type I nerve fibres indicated an average fibre diameter of about 3.35 μm across the range from basal to upper middle cochlear turns, and a 2.34 μm axonal diameter (Rosbe *et al.*, 1996; Glueckert *et al.*, 2005a). This gives a fibre-to-axon diameter ratio of 0.7, in agreement with values ranging from 0.63 – 0.8, depending on the fibre thickness (Behse, 1990). The relationship between fibre diameter and internodal length that was used in the model, however, was only valid for fibre diameters larger than 3.4 μm (Wesselink *et al.*, 1999). Since the largest diameter in the basal turn described in the Rosbe *et al.* (1996) study was 4.3 μm and the smallest in the upper middle turn 3.2 μm, the average, being 3.75 μm, was assumed in the ANF model.

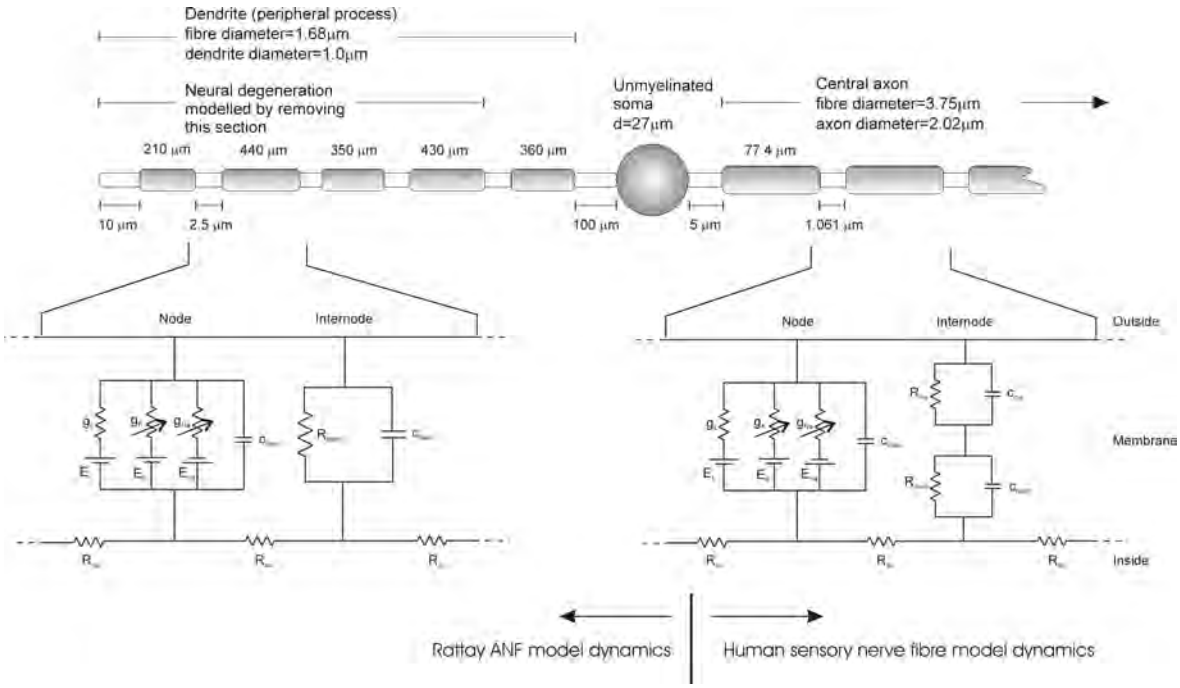

Figure 5.1: Representation of the human auditory nerve fibre. The dendrite is considered myelinated, with five internodes of variable lengths (Rattay *et al.*, 2001b). The myelin of these internodes is assumed a perfect insulator. The presomatic segment is divided into three sections (not indicated on sketch). Although the soma employs the Hodgkin-Huxley dynamics as described by Rattay *et al.* (2001b), its diameter is smaller than in the Rattay model. The axonal section employs the human sensory nerve fibre dynamics and morphometry and morphology. Unlike in the Rattay model, internodal lengths are considered constant and are shorter than in the Rattay model.

5.2.2 Modelling the degenerate nerve fibre

Retrograde neural degeneration, in which the dendrites are lost but the somas and axons survive, occurs in persons with profound sensory hearing loss (Nadol Jr, 1990; Schuknecht, 1993). The degree of retrograde neural degeneration depends on the severity of tissue alterations in the Organ of Corti during the original insult and concerns only Type I ANF's (Schuknecht, 1993).

Since not all ANFs are affected by retrograde degeneration, simulations were performed with three versions of the ANF model, simulating the effects of non-degenerated and increasingly degenerated nerve fibres respectively. A degenerate version of the ANF model, similar to Frijns, de Snoo and ten Kate (1996) and Briaire and Frijns (2006) was used to simulate the effect of neural degeneration, i.e. to simulate a nerve fibre with almost no peripheral process. This was effected by removing the first four nodal and internodal sections of the modelled ANF (refer to Figure 5.1). The first node in the degenerate version of the ANF model thus corresponded to node n_5 in Figure 5.2. An axon-only version was also modelled to simulate retrograde degeneration observed in long-term profoundly deaf persons (Schuknecht, 1993) by removing all dendritic nodes and internodes up to and including the soma in the ANF model.

5.2.3 The volume conduction cochlear model

The ANF model was coupled to a 3D spiralling finite element volume conduction model of the first one-and-a-half turns of the electrically stimulated human cochlea (Figure 5.2). For more details on the volume conduction model refer to Hanekom (2001b). Each of the nerve fibres present in the volume conduction model was described by the ANF model equations, where node n_1 in Figure 5.2 was the first node of the nerve fibre.

The cochlear model is designed to allow two possible electrode array positions, one medial and one lateral, relative to the modiolus. The Nucleus 24 straight array, which, after implantation, is positioned close to the outer wall of the cochlea (Miller, Abbas, Hay-McCutcheon, Robinson, Nourski and Jeng, 2004), is modelled with the lateral array, whereas the contour array, which lies close to the modiolus (Cohen *et al.*, 2003; Miller *et al.*, 2004) is modelled with the medial array. The straight array was

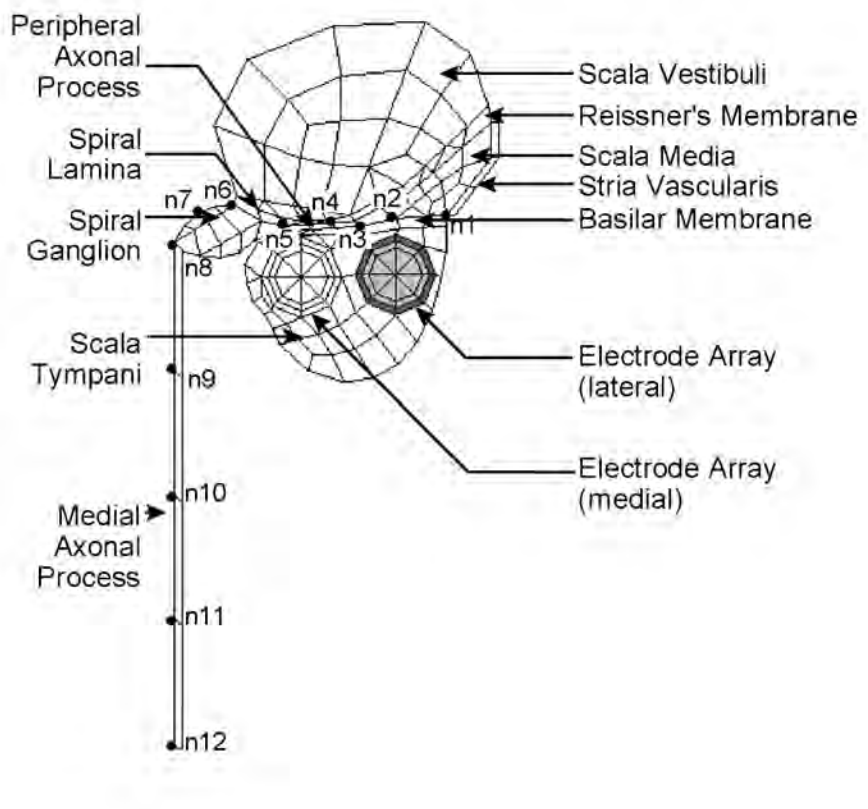

Figure 5.2: The two-dimensional finite element model geometry of a plane through the cochlea. The medial and lateral positions of the electrode array are shown as circular geometries towards the top of the scala tympani. The labels n_1 to n_{12} indicate the twelve locations (nodes) in the neural tissue where electrical potential values are calculated. (Figure used with permission from Hanekom, 2001b)

modelled with full-band electrodes and the contour array with half-band electrodes (Abbas and Miller, 2004; Miller *et al.*, 2004).

5.3 RESULTS

Simulations were performed in Matlab employing the same ODE solvers as discussed in previous chapters. Externally applied stimulation is incorporated through calculation of the external potential distribution inside the cochlea by the volume conduction cochlear model. The 3.75 μm diameter ANF fibre located in the basal cochlear turn was stimulated with a monopolar electrode configuration from either the con-

tour or straight electrode arrays at body temperature (37 °C). Stimulation pulses were square and monophasic-anodic. The computational methods used to calculate chronaxie time (τ_{ch}) values, as well as absolute (ARP) and relative refractory (RRP) periods have been described in Chapters 3 and 4. Results were compared for two classes of ANF fibres, i.e. a fibre containing only a transient sodium current (Na_t-fibre) and another fibre containing both a transient and a persistent sodium current (Na_p-fibre) at the axonal Ranvier nodes respectively. The results indicated that the Na_p-fibre best predicted Type I ANF excitation behaviour and hence only these results will be tabulated, while the results for the Na_t-fibre will only be discussed.

5.3.1 Strength-duration relationships

Chronaxie time (τ_{ch}) values were calculated for both fibre classes for stimulation with the contour and straight arrays respectively. In general τ_{ch} values decreased with a modelled increase in fibre degeneracy as shown in Table 5.1. Calculated τ_{ch} values for contour and straight arrays predicted about 10% higher values in the former case compared to the latter for non-degenerate and degenerate fibres, while values for the axon-only fibres were similar. For an axon-only fibre the Na_p-fibre had a τ_{ch} value of about 111 μs compared to a value of 86.1 μs for the Na_t-fibre, irrespective of the electrode array used. Values were also 50 – 60% higher for the Na_p-fibre compared to the Na_t-fibre.

Simulations predicted a rheobase current of 0.87 mA for a non-degenerate Na_p-fibre, 0.88 mA for a degenerate and 0.89 mA for an axon-only fibre when stimulated with the contour array. Rheobase current values for straight array stimulation were about twice higher compared to contour array stimulation. Corresponding values for a Na_t-fibre were about 10% lower for contour array and about 20% higher for straight array stimulation.

5.3.2 Refractory periods

Simulated ARP values for all versions of the Na_t-fibres and Na_p-fibres compared well to those of general sensory nerve fibres (Table 4.4), being 0.8 – 0.9 ms irrespective of the stimulation electrode array used (Table 5.1).

Table 5.1: Simulated characteristics of a human Type I ANF in the basal cochlear turn, using monopolar-monophasic stimulation for the Nucleus 24 straight and contour electrode arrays respectively. Values shown are for ANFs containing both a transient and a persistent sodium current at the axonal Ranvier nodes. Three versions of the ANF were modelled, indicating the degree of degeneracy of the ANF. All simulations were performed at 37 °C.

Parameter	**Specifications**	**Human ANF model (contour array)**	**Human ANF model (straight array)**
Chronaxie (μs)	Non-degenerate ANF	261.0	235.8
	Degenerate ANF	240.0	220.5
	Axon-only ANF	110.0	111.9
Conduction velocity (μs^{-1})	Non-degenerate ANF	2.09	2.15
	Degenerate ANF	2.05	1.95
	Axon-only ANF	6.54	5.15
ARP (ms)	All ANF versions	0.8	0.9
RRP (ms)	Non-degenerate ANF	4.6	4.5
	Degenerate ANF	4.4	4.1
	Axon-only ANF	4.3	4.2

Simulated RRP values differed, depending on the fibre used as well as the stimulation array used. Values for axon-only, degenerate and non-degenerate Na_p-fibres are listed in Table 5.1. For a non-degenerate fibre the RRP value was 11% longer compared to a degenerate fibre when stimulated with the straight array, and 6% longer when stimulated with the contour array, while values were about 3% longer for stimulation with the latter array compared to the former. For a Na_t-fibre contour array stimulation predicted about 5% longer RRP values compared to the straight array, while values were about 31% shorter compared to those for a Na_p-fibre. Values for a non-degenerate fibre were about 6% longer than for degenerate and axon-only fibres.

5.3.3 Conduction velocities

Conduction velocities and latencies were determined for monopolar stimulation with a monophasic pulse of 0.5 ms. Calculated conduction velocity (v_c) values for an axon-only Na_p-fibre were 24.5 m.s^{-1} (contour array) and 19.3 m.s^{-1} (straight array), and 12.8 m.s^{-1} (contour array) and 10.4 m.s^{-1} (straight array) for a Na_t-fibre compared to 9.0 m.s^{-1} for a similar general sensory nerve fibre stimulated externally. To aid comparison of v_c values between fibres of different diameter, it is customary to list

these values in terms of v_c values per fibre diameter (Wesselink *et al.*, 1999). Hence, for a Na_p-fibre, v_c values per fibre diameter are listed in Table 5.1. For a degenerate Na_p-fibre, v_c values were about 69% slower compared to stimulation of an axon-only fibre for contour array stimulation and about 62% slower for straight array stimulation. Non-degenerate Na_p-fibre v_c values were 2% faster compared to degenerate fibres for contour array stimulation and about 10% faster for straight array stimulation. Both non-degenerate and degenerate Na_t-fibre v_c values were similar to Na_p-fibre v_c values under the same stimulation conditions.

ANF performance is not measured in terms of v_c values and hence these values were translated into propagation times. AP propagation time is defined as the time taken by the AP to travel the length of the modelled ANF. Na_p-fibre AP propagation times for full, degenerate and axon-only fibres respectively were 0.41 ms, 0.23 ms and 0.05 ms for contour array stimulation and 0.40 ms, 0.24 ms and 0.065 ms for straight array stimulation. Propagation times for Na_t-fibres were 19% (non-degenerate), 32% (degenerate) and 257% (axon only) longer compared to Na_p-fibres for contour array stimulation. Corresponding propagation times for straight array stimulation were about 7% shorter than for contour array stimulation.

5.3.4 Mean latencies

Spike latency is defined as the time latency between stimulus onset and maximum AP amplitude, while mean latency is the mean of all the spike latencies measured for a specific stimulus intensity (Miller *et al.*, 1999b). In a deterministic model the mean latency would therefore compute to the spike latency. Mean latencies for an AP originating on the axon of a non-degenerate Na_p-fibre situated close to the stimulating electrodes in the basal cochlear turn for stimulation with the straight and contour array respectively are shown in Figure 5.3. Results for the degenerate case were similar to those of the non-degenerate fibre. Mean latencies decreased with an increase in stimulus intensity, ranging from about 0.48 ms at threshold intensity to about 0.24 – 0.25 ms at the maximum intensity calculated. In general stimulus intensities were lower for the contour array than for the straight array.

Mean latencies of APs originating on the dendrite of a fibre are shown in Figure 5.4 for non-degenerate and degenerate Na_p-fibres. All conditions were the same as for results

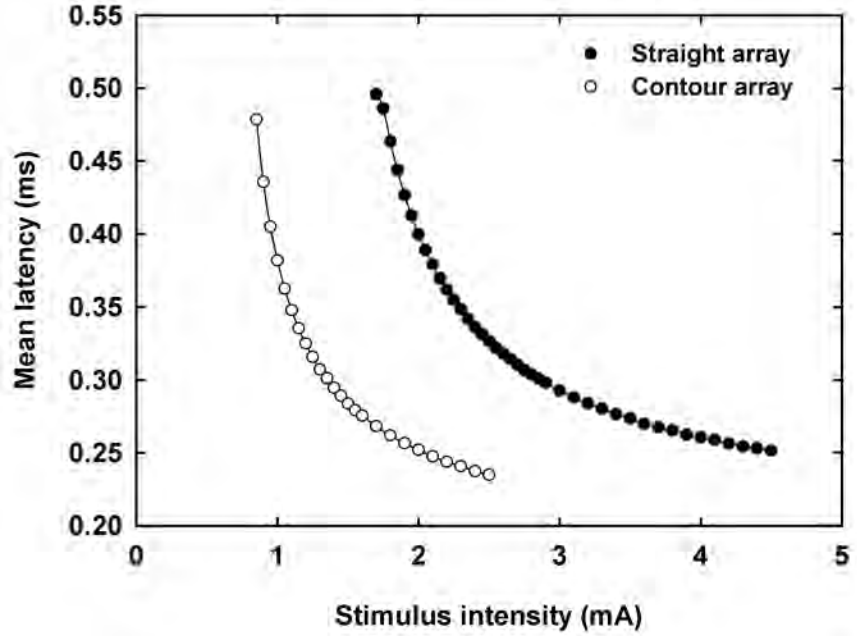

Figure 5.3: Calculated mean latencies for a non-degenerate Na_p-fibre stimulated with the straight and contour arrays respectively. The modelled fibre was situated close to the stimulating electrode in the basal turn. Open markers indicate results for contour array stimulation and closed markers results for straight array stimulation. Results for a degenerate fibre were similar to the non-degenerate case and are not shown.

shown in Figure 5.3. Mean latencies tended to decrease with an increase in retrograde degeneracy, ranging between 0.5 – 0.7 ms for a degenerate fibre compared to the range of 0.63 – 0.87 ms for a non-degenerate fibre. In contrast to the trend towards straight array stimulation, latencies calculated with contour array stimulation decreased to a minimum, after which they started to increase again, possibly suggesting a decrease in v_c with a stimulus intensity increase.

Double-peak evoked compound action potential (ECAP) responses have been observed in cats and humans (see for example studies by Van den Honert and Stypulkowski, 1984; Lai and Dillier, 2000). In these studies it has been suggested that the double positive peak response is indicative of the existence of surviving dendrites. The first positive peak (*P1*) originates from axonal excitation, while the second peak (*P2*) is due to dendritic excitation. The difference in latency between the two peaks can hence serve as an indication of propagation time across the soma. Similarly, the

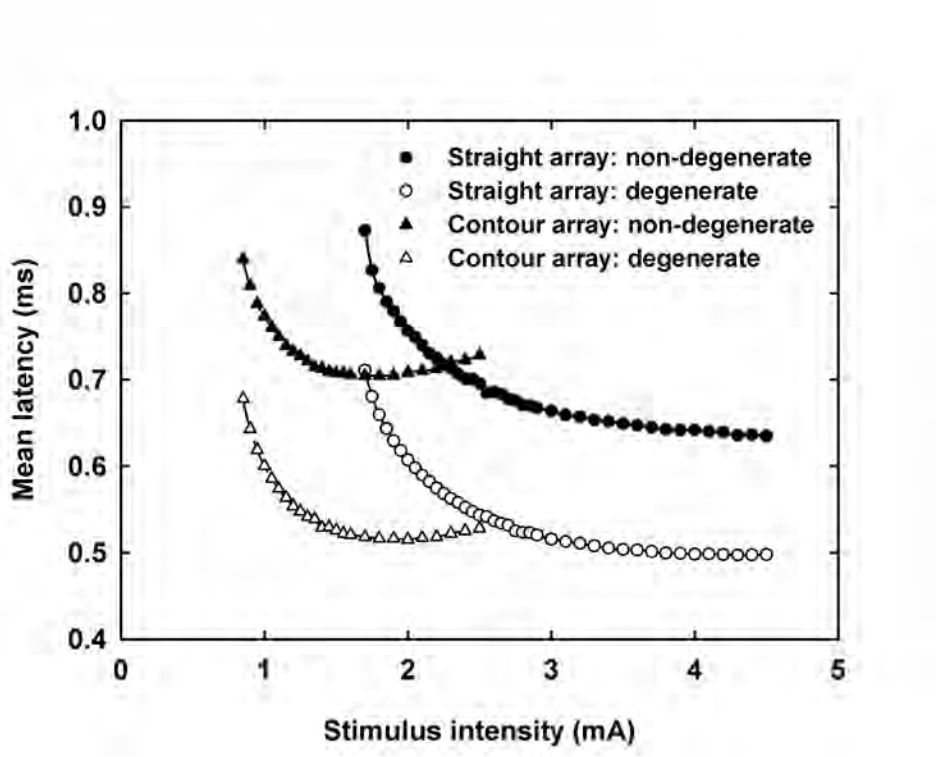

Figure 5.4: Mean latencies calculated for an AP originating from the dendritic process of non-degenerate and degenerate Na_p-fibres respectively. Fibres were situated in the basal cochlear turn close to the stimulating electrode of the straight and contour arrays respectively. Closed markers indicate non-degenerate fibre results and open markers the results for degenerate fibres. Results for straight array simulation are indicated with circles and solid lines, and contour array results with triangles and dashed lines.

propagation times across the soma can be calculated from the difference in latencies between Figures 5.3 and 5.4. Propagation times thus calculated for the contour array ranged between 0.361 and 0.493 ms for non-degenerate and 0.199 and 0.293 ms for degenerate ANFs. Propagation times calculated with the straight array were shorter compared to those of the contour array and ranged between 0.341 and 0.381 ms for non-degenerate and 0.192 and 0.238 ms for degenerate ANFs.

Results for the Na_t-fibre followed the same trends as for the Na_p-fibre. However, similar to the longer propagation times calculated for the Na_t-fibre compared to the Na_p-fibre, mean latencies where longer than for the Na_p-fibre, and are hence not shown.

5.4 DISCUSSION AND CONCLUSION

No experimental results exist regarding the fall and rise times, as well as the conduction velocity of the propagating action potential in ANFs. Instead, these fibres are classified in terms of temporal characteristics; including ARP and RRP properties, strength-duration behaviour and mean latencies (see for example a review by Abbas and Miller, 2004). All these characteristics depend, *inter alia*, on the type and strength of stimulation pulse, the electrode configuration and electrode-fibre distance (Abbas and Miller, 2004). In this study stimulation of the modelled cochlea was performed with two different Nucleus 24 electrode arrays in monopolar configuration, with the contour array positioned closer to the axonal part of the nerve fibres than the straight array. Stimulation pulses were square monophasic and anodic.

Stimulation in cochlear implants is typically in the form of pulse trains or continuous stimulation. The refractory properties of the neural membrane play an important role in the choice of stimulation used (Abbas and Miller, 2004). Firstly, it places a lower limit on the interphase / interpulse interval, raising the threshold stimulus intensity needed to elicit further responses during the RRP, and secondly, it places an upper limit on the stimulus rate used (Abbas and Miller, 2004). Mean ARP values between 0.33 ms (Miller *et al.*, 2001a) and 0.7 ms (Cartee *et al.*, 2000) and a mean recovery time constant of about 0.41 ms were estimated for cat auditory fibres (Miller *et al.*, 2001a) and an RRP of up to 5 ms (Cartee *et al.*, 2000; Abbas and Miller, 2004). ECAP studies on humans suggest an ARP value larger than 0.5 ms and a RRP value around 5 ms (Brown *et al.*, 1990). These measured human values are 44% shorter for the ARP and 15% – 23% longer for the RRP than the present model for a degenerate Na_p-fibre predicts, depending on the stimulation electrode array used. The Na_p-fibre also predicted the measured results better than the Na_t-fibre. It therefore seems that Type I ANF fibres may contain both transient and persistent sodium current components.

Although the somas and axons of the Type I ANF fibre degenerate at a slower rate than the dendrites, SEM studies of long-term profoundly deaf persons show a sharp decrease in the number of surviving fibres, compared to shorter term deaf persons (Schuknecht, 1993). Model predictions suggested that retrograde degeneration may not influence the ARP of ANFs, but this prediction has not previously been studied experimentally. The simulated RRP results for a non-degenerate fibre were longer than

for degenerate and axon-only fibres, possibly suggesting that longer-term deaf persons may benefit from implants employing faster stimulation rates than shorter-term deaf persons.

Latency measurements on normal hearing cats and cats in which the dendrites and somas were removed during a cochlear laminectomy showed a double-peak response in the normal hearing cats, while in the laminectomated cats only the first response peak appeared (Van den Honert and Stypulkowski, 1984). Van den Honert and Stypulkowski (1984) proposed that the former reflected peripheral dendritic excitation and that the shift in latency indicated a shift in excitation to a more centrally located site along the fibre. More recent ECAP studies on cats also suggested this proposition (Miller *et al.*, 1998; Miller *et al.*, 1999b; Miller *et al.*, 1999a; Miller *et al.*, 2001a). NRT measurements in human subjects implanted with the Nucleus 24 arrays also indicated the existence of similar response waveforms having either single positive or double positive peaks (Lai and Dillier, 2000). The NRT waveform is characterized by a negative (*N1*) peak, followed by the positive peak(s) (*P1* and *P2*). For a single positive peak waveform, the *N1* peak occurred around 0.3 – 0.4 ms and the *P1* peak around 0.6 – 0.7 ms. In the double positive peak responses, the *N1* peak occurred at times too short to measure with the NRT system (< 0.11 ms), while the *P1* and *P2* peaks occurred around 0.4 – 0.5 ms and 0.6 – 0.7 ms respectively. Calculated latencies for the single-peak case were hence ~ 0.3 ms. For the double-peak case it was ~ 0.4 ms and ~ 0.7 ms, while the resulting propagation times range between 0.2 and 0.3 ms. Lai and Dillier (2000) concluded that the double-peak response indicated the existence of almost intact ANF fibres, while the single-peak response might be due to retrograde degeneration. Latencies calculated for single fibres with the present human ANF Na_p-fibre model for degenerate fibres agreed well with these experimental human results. Predicted results were in agreement with the suggestion that longer latencies indicate the presence and dendritic stimulation of more intact ANFs, owing to the additional time it takes the AP to propagate along the fibre.

The strength-duration function gives the relationship between the threshold stimulus current necessary to excite a fibre and the stimulus duration. Strength-duration behaviour is characterised by the rheobase current and chronaxie time. Strength-duration curves measured for normal and damaged cat auditory nerve fibres show that for the damaged fibres, where only the axons are left intact, thresholds at short pulse durations are lower than for the normal fibres (Van den Honert and Stypulkowski, 1984).

This is most probably due to the fact that the damaged fibres are only excited in the axonal (central) part of the fibre, while for normal fibres excitation could occur either peripherally or centrally (Van den Honert and Stypulkowski, 1984). Simulations with the present model predicted higher rheobase values for axon-only fibres compared to degenerate and non-degenerate fibres. This can be attributed to the model itself. In Section 5.2 mention was made of the fact that the relationship between fibre diameter and internodal length that was used in the axonal part of the modelled fibre was only valid for fibre diameters larger than 3.4 μm. The dendritic diameter is only 1.0 μm, and hence the dendritic section of the fibre could not be replaced with the general sensory nerve fibre dynamics. Because of the difference in dynamics between the original Rattay *et al.* (2001b) model and the general sensory nerve fibre model, it is expected that the present ANF fibre model's excitation behaviour will differ from a model where the squid dynamics of the dendritic as well as the somal sections are also replaced with human dynamics.

Van den Honert and Stypulkowski (1984) also reported significantly shorter (118.0 μs versus 276.0 μs) chronaxie times for fibres of which the dendrites and somas were removed (leaving only the axons intact) compared to normal functioning fibres, indicating axonal excitation in the former. In both cases the fibres are electrically stimulated. Although the chronaxie time of about 111.0 μs for an axon-only simulated Na_p-fibre was much shorter compared to a similar general sensory human fibre, chronaxie times followed the trend of decreasing as the modelled fibre became progressively more degenerated.

According to Abbas and Miller (2004), chronaxie times depend on the electrode-axon distance. A closer separation may lead to a decrease of the strength-duration time constant and thus shorter chronaxies. The trend predicted by the present model was in contrast to the experimentally observed trend in that the chronaxie times for non-degenerate and degenerate fibres increased when the electrode-fibre distance was decreased, confirming the shortcoming in the model regarding dendritic modelling discussed previously.

In conclusion it therefore seems possible to modify the Hodgkin-Huxley equations to describe action potentials generated in the Ranvier node of a human sensory nerve fibre and apply these modification to create more realistic neural models of the electrically stimulated human auditory system. Comparison between predicted and experimentally

measured results of Type I ANF fibres also suggested the existence of similar sodium ionic membrane currents than present in general sensory nerve fibres. However, the squid-based dynamics of the dendritic and somal model sections need to be replaced with human dynamics to account fully for experimentally observed ANF excitation behaviour.

The next chapter takes a look at the development of a simple method to approximate the calculation of ECAPs. The output of the ANF model is a neural excitation profile at the location of the ANFs and is used as input to the method. ECAP profile widths at the location of the stimulating electrode array, as well as the estimated stimulus attenuation inside the cochlea can thus be determined.